Heliyon 10 (2024) e31317

Contents lists available at ScienceDirect

Heliyon

journal homepage: www.cell.com/heliyon

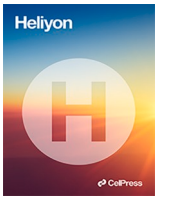

Research article

Novel ultrasensitive automated kinetic exclusion assay for measurement of plasma levels of soluble PD-L1, the predictive and prognostic biomarker in cancer patients treated with immune checkpoint inhibitors

Ibrahim A. Darwish [a,*], Waleed Alahmad [b], Rajendran Vinoth [c,d]

[a] Department of Pharmaceutical Chemistry, College of Pharmacy, King Saud University, P.O. Box 2457, Riyadh, 11451, Saudi Arabia
[b] Department of Chemistry, Faculty of Science, Chulalongkorn University, Bangkok, 10330, Thailand
[c] Electrodics and Electrocatalysis Division, CSIR-Central Electrochemical Research Institute (CECRI), Karaikudi, Tamil Nadu, 630003, India
[d] Academy of Scientific and Innovative Research (AcSIR), Ghaziabad, 201002, India

ARTICLE INFO

Keywords:
Cancer
Predictive and prognostic biomarkers
PD-L1
Biosensor
KinExA

ABSTRACT

Recently, the blood plasma or serum levels of soluble programmed death protein 1 (PD-L1), but not tissue PD-L1 expression level, have been proposed as an effective predictive and prognostic biomarker in patients treated with immune checkpoint inhibitors for different types of cancers. The quantification of soluble PD-L1 in blood will provide a quick evaluation of patients' immune status; however, the available assays have limitations in their sensitivity, reproducibility, and accuracy for use in clinical settings. To overcome these problems, this study was dedicated to developing an ultrasensitive automated flow-based kinetic exclusion assay (KinExA) for the accurate and precise measurement of soluble PD-L1 in plasma. The assay was developed with the assistance of KinExA™ 3200 biosensor. In this assay, PD-L1 in its calibrator or plasma sample solution was pre-equilibrated with anti-PD-L1 monoclonal antibody. The equilibrated mixture solution was then passed rapidly over PD-L1 protein that has been coated onto polymethylmethacrylate beads consolidated as a microcolumn in the observation cell of the KinExA™ biosensor. The free anti- PD-L1 antibody was bound to the immobilized PD-L1, however, the unbound molecules were removed from the beads microcolumn by flushing the system with phosphate-buffered saline. Fluorescein-labeled secondary antibody was passed rapidly over the beads, and the fluorescence signals were monitored during the flow of the labeled antibody through the beads. The calibration curve was generated by plotting the binding percentages as a function of PD-L1 concentrations in its sample solution. The working range of the assay with very a good correlation coefficient on a 4-parameter equation ($r = 0.9992$) was 0.5 – 100 pg mL^{-1}. The assay limit of detection and quantitation were 0.15 and 0.5 pg mL^{-1}, respectively. The recovery values of plasma-spiked PD-L1 were in the range of 96.4–104.3 % (±3.7–6.2 %). The precision of the assay was satisfactory; the values of the coefficient of variations did not exceed 6.2 % for both intra- and inter-day precision. The automated analysis by the proposed KinExA facilitates the processing of many specimens in clinical settings. The overall performance of the proposed KinExA is superior to the available assays for plasma levels of soluble PD-L1. The

* Corresponding author.
E-mail address: idarwish@ksu.edu.sa (I.A. Darwish).

https://doi.org/10.1016/j.heliyon.2024.e31317
Received 17 November 2023; Received in revised form 14 May 2024; Accepted 14 May 2024
Available online 15 May 2024
2405-8440/© 2024 The Authors. Published by Elsevier Ltd. This is an open access article under the CC BY-NC license (http://creativecommons.org/licenses/by-nc/4.0/).

proposed assay is anticipated to have a great value in the measurement of PD-L1 where a more confident result is needed.

1. Introduction

Immunotherapy of malignancies with immune checkpoint inhibitors (ICIs) has gained significant attention to oncologists. ICIs work by blocking the checkpoint proteins from binding to their partner proteins. This prevents the "off" signal from being sent, allowing the T cells to kill cancer cells. This checkpoint mechanism ensures the tight balance between protective and damaging impacts of the immune pathways and can therefore be exploited using specific antibodies for anti-tumor immunity [1]. Programmed cell death protein 1 (PD-1) is a transmembrane surface protein expressed on tumour-infiltrating immune cells. The main ligand for PD-1 protein is the programmed death ligand (PD-L1), expressed on antigen-presenting cells and tumour cells. PD-1 and PD-L1 are interacting immune-checkpoint proteins that negatively regulate the adaptive antitumour immune response [2]. PD-L1 expression enables tumour cells to evade immune surveillance [2,3]. Thus, immunotherapy by ICIs has been attempted and found promising way for the treatment of many solid tumors [4,5]. Immunotherapy with monoclonal antibodies against the PD-1/PD-L1 axis has changed the treatment landscape for advanced-stage forms of many cancers, including melanoma, lung cancer, breast cancer, kidney cancer and many others [3]. However, these antibodies can promote antitumour immunity and thus eliminate tumour cells and provide a strong rationale to the further development of PD-L1 expression as a predictive biomarker of response to anti- PD-1 or anti- PD-L1 antibodies [6]. While favourable long-term outcomes with these therapies compared to previous standard approaches, only 10–40 % of patients obtain dramatic responses [7] and even fewer will have long-term disease remission. Additionally, the five-year overall survival rate of ICIs treatment ranges from 15.5 % to 41 % in advanced malignancies [8,9]. Therefore, developing single or multiple biomarkers for identifying groups of patients who could benefit from ICIs is critical.

To date, various biomarkers, including tumor tissue PD-L1 expression, tumor mutation burden, tumor neoantigen burden, high microsatellite instability, deficient mismatch repair, tumor-infiltrating lymphocytes, T-cell receptor clonality, effector T-cell gene signature, DNA damage and repair genes, and intestinal microbiota, have been proposed as predictive and prognostic biomarkers in cancer patients who receive ICIs therapy [7–10]. The tissue PD-L1 expression was first approved as a predictive biomarker for the clinical responses to PD-1 or PD-L1 immunotherapy in patients with a variety of tumour types [11,12]. Accordingly, multiple assays designed to assess PD-L1 expression have been approved for clinical use by the FDA [13–15]; however, these assays showed discrepancies in their results even of the same samples, leading to unconfident results, which might have important implications for patients in terms of their eligibility to receive anti- PD-1 or anti- PD-L1 immunotherapy. Additionally, the other biomarkers lack standardization and exhibit high variability across tumor types [16]. Based on these observations, these tumor-derived biomarkers are not very reliable for accurate prediction. Since the immune response is controlled by the properties of both the tumour and the immune system, biomarkers that reflect immune properties are needed.

Recent studies revealed that soluble PD-L1 is detectable in blood plasma or serum, and its levels abnormally increase in patients with cancer [17–27]. Also, the level of soluble PD-L1, but not tissue PD-L1 expression level, has been proposed as an effective predictive and prognostic biomarker in patients treated with ICIs for different types of cancers [17–27]. Recent studies have developed a few assays to facilitate the detection of soluble PD-L1 in the plasma or serum of cancer patients who receiving ICIs therapy [28–32]. These assays were metal–organic framework-enhanced enzyme-linked immunosorbent assays, ELISA [29], localized surface plasmon resonance (SPR) biosensor [30], surface-enhanced Raman scattering, SERS [31,32], and magnetic chemiluminescent immunoassay, CLIA [33]. These assays, although they offered high sensitivities, still suffered from major drawbacks. ELISA and CLIA involved multiple steps, thus the overall process is time-consuming, and the precision of results was low. SPR is typically affected by the sample matrix components because of the non-specific binding or adsorption of molecules to the sensor surface, leading to false-positive signals. This is particularly problematic when analyzing complex blood samples. SERS involved complicated procedures for the fabrication and functioning of the sensor chip. In addition, the signals can exhibit significant variability because of variations in the surface enhancement factors, non-uniformity of the nanostructures, and fluctuations in laser power or measurement conditions. These factors can make the accurate quantitative analysis of PD-L1 seriously challenging. Furthermore, in these solid phase assays, the PD-L1 molecules in the samples are adsorbed onto the solid surfaces, leading to alteration in their binding kinetics. For these reasons, further research is needed to develop a novel method that surpasses the limitations of current techniques for the quantitation of PD-L1 in blood.

Kinetic-exclusion assay (KinExA)-assisted with KinExA™ biosensor has emerged as a significant technological advancement in the field of biomolecular analysis, offering unique features. This system enables the direct interfacing of ligand-antibody binding to a fluorescent signal transducer. KinExA enables the real-time determination of true-solution-based binding affinities and kinetics of molecular interactions [34]. In previous studies [35–38], our laboratory have developed successful KinExA-based assays for quantitative analysis of diverse analytes, showcasing advantages over conventional immunoassays like ELISA. These advantages include the elimination of immobilization effects, overcoming mass transport limitations, and providing improved performance. Unlike measurements in solid surface-based assays, the analyte molecules in KinExA are unmodified, enabling real-time monitoring of binding events, providing real kinetic information about the interacting molecules and faster analysis. Additionally, KinExA has been shown to be 10–1000 fold more sensitive than ELISA, even when using the same reagents [39]. Furthermore, KinExA analysis is conducted in an automated and high-throughput manner, facilitating the screening of a large number of samples. Furthermore, KinExA requires small sample volumes, making it suitable for the analysis of precious or limited samples [39].

The present study describes, for the first time, the development of automated ultrasensitive KinExA for the measurement of plasma levels of PD-L1. The assay offers the inherent advantages of KinExA technology and overcomes the drawbacks/limitations of the other existing assays for soluble plasma level of PD-L1.

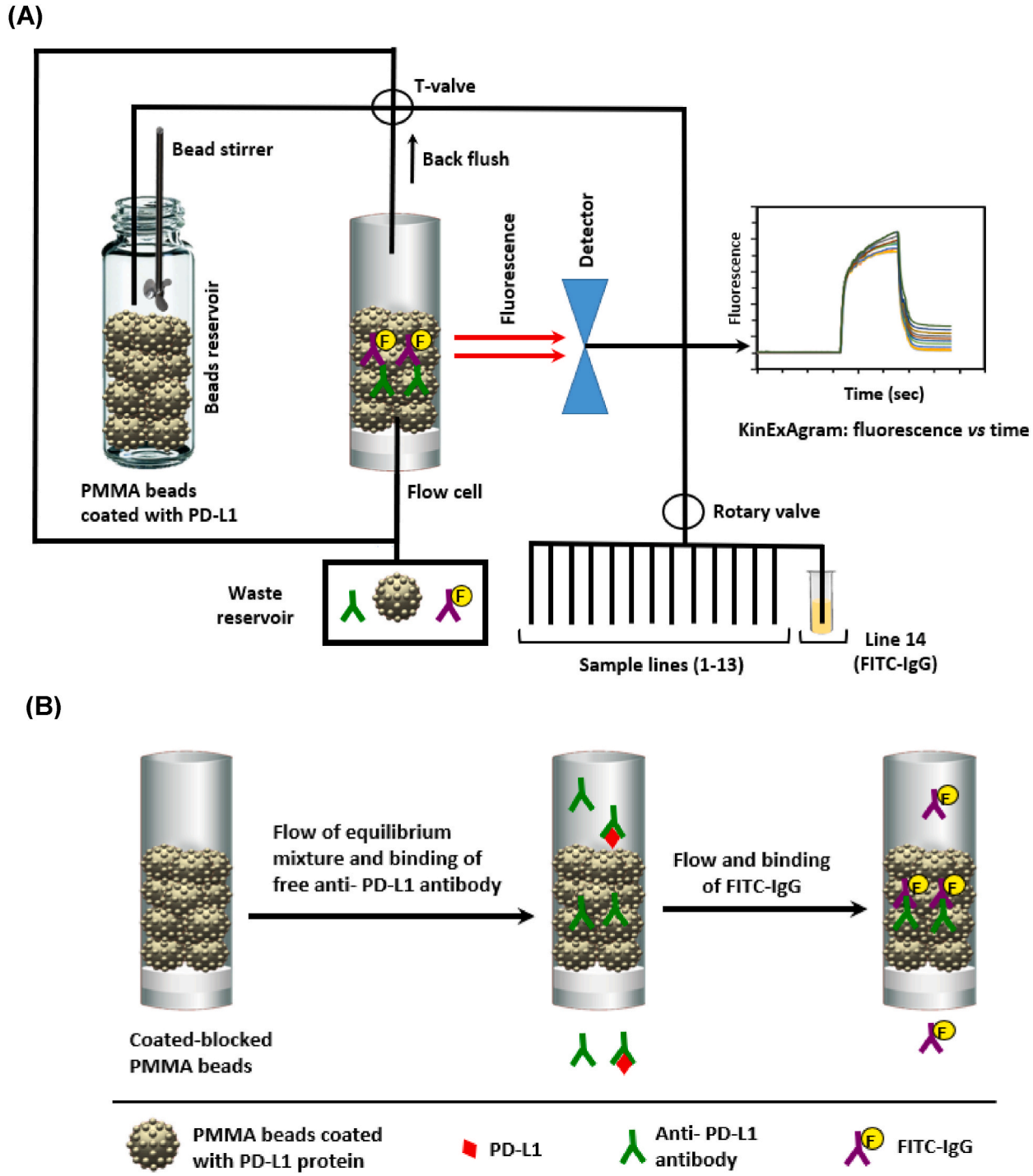

Fig. 1. A schematic representation of the operation of the Kinetic Exclusion Assay (KinExA) biosensor (A) and principles of KinExA for the programmed death protein 1, PD-L1 (B). Beads are coated with PD-L1 protein and a pre-equilibrated mixture of PD-L1 (in the samples) and anti PD-L1 antibody was allowed to pass through the beads. Fluorescein-labeled second antibody (FITC-IgG) was passed through the bead's column, and the fluorescence signal is continuously monitored during flow by a photodiode array detector facing the flow cell of the instrument and the signals are recorded.

2. Experimental

2.1. Instruments

KinExA™ 3200 biosensor was a product of Sapidyne Instruments Inc. (Boise, ID, USA). Incubator (Model MINI/18: Genlab Ltd., Widnes, UK). Nutating mixer was a product of Taitec (Saitama-ken, Japan). Microprocessor pH meter (Model BT-500: Boeco, Hamburg, Germany). Biofuge centrifuge (Z206A: Hermle Labortechnik, Germany). Vortex (Clifton cyclone CM1: Weston, England). Biomedical freezer (MDF-U5312: Sanyo Onoda, Japan). Milli-Q water purification system (Millipore Ltd., Bedford, USA).

2.2. Materials

Recombinant human PD-L1 protein and anti- PD-L1 antibody were obtained from R&D systems Inc. (Minneapolis, MN, USA). Bovine serum albumin (BSA) and fluorescein-isothiocyanate conjugate of anti-human IgG (FITC-IgG) were obtained from Sigma-Aldrich LLC (California, CA, USA). Polymethylmethacrylate (PMMA) beads (140–170 mesh, 98 μm) were obtained from Sapidyne Instruments Inc. (Boise, ID, USA). Human plasma was obtained from Blood Bank of King Saud University Medical City (Riyadh, Saudi Arabia). All other chemicals used throughout the work were of analytical grade.

2.3. Techniques and procedures

2.3.1. Coating of PD-L1 protein onto PMMA beads

PMMA dry beads (200 mg contained in a vial) were individually coated with PD-L1 protein. The coating solution consisted of 1 mL of phosphate buffered saline (PBS) containing 0.2 mg mL^{-1} of PD-L1. The bead vials with the coating solution were placed on a nutating mixer at 37 °C for 1 h. Afterward, the bead vials were taken off the mixer, allowing the beads to settle at the bottom of the vials. The supernatant was aspirated, and 1 mL of BSA solution (2 %, w/v, in PBS) was added to each vial. The bead vials were then returned to the nutating mixer for 0.5 h at 37 °C to block any remaining protein-binding sites on the coated beads. Finally, the coated beads were collected and stored in a refrigerator at 4 °C. The coated and blocked beads remained stable for at least 2 weeks.

2.3.2. Analysis on KinExA™ 3200 biosensor

The setup of KinExA™ 3200 biosensor is illustrated in Fig. 1A. It consists of 14 sampling lines, with 12 lines dedicated to automatically dispensing the samples from test tubes containing PD-L1 samples (calibrator solutions or spiked plasma) at concentrations range of 0.05 − 250 pg mL^{-1} in PBS with 0.1 % BSA). The 13th line is used for dispensing a blank solution (zero concentration of PD-L1), while the 14th line is used for dispensing the FITC-IgG solution. The coated and blocked PMMA beads were transferred with 30 mL of PBS to the bead's reservoir of the instrument. The beads were loaded with an initial dilution of the beads using 30 mL of PBS. The bead's reservoir is featured with a stirrer to ensure the uniform distribution of beads upon charging the beads to the flow cell to build up a microcolumn of beads. The beads were charged twice to ensure an appropriate height of a bead column, which could be monitored by a camera inside the flow cell. The column height could be adjusted by modifying either the flow time or the flow volume aspirated from the bead reservoir. By using a flow volume of 583 μL at a flow rate of 1 mL min^{-1}, the desired bead column height (approximately 4 mm) was achieved consistently. The bead columns produced under these conditions were identical and reproducible. The instrument automatically withdraws samples with negative pressure in sequence starting from line 1 to line 13. Aliquots (500 μL) of a pre-equilibrated (~10 min) PD-L1 sample solution containing anti- PD-L1 antibody (20 ng mL^{-1}) were aspirated at a flow rate of 0.25 mL min^{-1} and passed over the freshly generated bead column for a duration of 120 s. After each sample aspiration, a buffer wash was performed using 125 μL of PBS for 30 s to remove any remaining unbound PD-L1 or antibody molecules from the bead column. One millilitre of FITC-IgG solution (0.2 μg mL^{-1} in PBS with 0.1 % BSA) was withdrawn and passed over the bead column at a flow rate of 0.25 mL min^{-1}. Unbound FITC-IgG molecules were subsequently removed by passing 1.5 mL of PBS through the beads for 90 s at a flow rate of 1 mL min^{-1}. The photodiode camera installed in the flow/observation cell was continuously monitoring the signals. Data acquisition (started immediately, in all cases, following the building up of the microcolumn of beads) and instrument control were accomplished via a computer interfaced to the KinExA instrument using software (KinExA Pro 20.0.1.26) provided by with the instrument by Sapidyne Instruments, Inc. data was exported into SlideWrite (version 2.1, Advanced Graphics, Inc., Carlsbad, CA) and exploiting curve-fitting by 4-parameter equation:

$$F = F_0 - \{(F_0 - F_1)[\text{PD-L1}] / (IC_{50} + [\text{PD-L1}])\}$$

Where F is the fluorescence signal at a definite known concentration of PD-L1, F_0 is the fluorescence signal at zero concentration of PD-L1, F_1 is the fluorescence signal at the saturating concentration of PD-L1, and IC_{50} is the PD-L1concentration that produces a 50 % inhibition of the signal. The concentrations of PD-L1 in the samples were obtained by interpolation on the calibration curve.

3. Results and discussion

3.1. Description of KinExA

The setup of the KinExA™ 3200 system and operational steps of KinExA for PD-L1 are illustrated in Fig. 1. In this assay, samples

containing varying concentrations of PD-L1 and a fixed limited amount of anti- PD-L1 antibody are pre-equilibrated and applied to a bead microcolumn. The microcolumn consisted of PMMA beads coated with PD-L1 protein. The samples were drawn onto the bead microcolumn for a brief period, allowing the antibody molecules with free binding sites to interact with the immobilized PD-L1 protein. Any remaining antibody molecules in the column were then removed by a buffer wash. Next, FITC-IgG was introduced over the bead column, where the antibody molecules had been captured by PD-L1 coated onto the PMMA beads. The amount of FITC-IgG retained on the beads was inversely related to the quantity of PD-L1 in the sample solution. Following this step, a wash was performed to eliminate any excess unbound FITC-IgG on the bead column. The fluorescence intensity was measured using the photodiode included in the KinExA™ 3200 system. The fluorescence signals monitored were those obtained at the end of the analysis run, after the unbound FITC-labeled antibody had been washed away from the bead column. The detector responses versus time are represented as a KinExAgrams (Fig. 1).

3.2. Optimization of KinExA conditions

3.2.1. Optimization of KinExA signals

Initial experiments were conducted to assess the "net signal" produced by the KinExA biosensor when a definite concentration of free anti- PD-L1 antibody binds to a solid phase (PMMA coated with PD-L1). The sensor's "100 % signal" corresponds to the voltage obtained when all the binding sites on the antibody molecule in solution are in the free form and fully available for binding to the PD-L1 coated onto the PMMA beads. Conversely, the signal obtained for non-specific binding represents the voltage recorded when there are no binding sites in the solution (only sample buffer and labeled secondary antibody). By subtracting the non-specific binding signal from the 100 % signal, we obtained the net analytical signal. Maintaining a constant background signal was crucial for obtaining reproducible results since the processed signal relied on the difference between the background and final signal. An increase in background signal often occurs due to reagent adsorption onto the column wall and inadequate washing. To address this issue, we implemented an overnight washing step of the inlet lines with PBS containing Tween-20 prior to the analysis, effectively reducing the background signal.

3.2.2. Selection of concentrations of PD-L1 protein and anti- PD-L1 antibody

According to the principles of KinExA (Fig. 1), achieving of the highest possible sensitivity is limited only by the antibody's affinity to PD-L1 and not by the instrument itself. Additionally, the rapid flow of the pre-equilibrated mixture of PD-L1 and its antibody over the immobilized PD-L1 in the observation cell prevents the dissociation of immune complexes during passage. Therefore, the immobilized PD-L1 served as a tool for separation and not as an effective competitor for antibody binding sites. This enables the detection of only free antibody molecules with unoccupied binding sites in the equilibrium mixture, leading to higher sensitivity. In KinExA, even a very low concentration of antibody can generate adequate signal strength through accumulation from continuous sample flow.

To determine the best concentration of anti- PD-L1 antibody, a set of experiments was conducted using varying concentrations of antibody ($5 - 20$ ng mL^{-1}), and the IC_{50} value was determined in each case. The obtained IC_{50} values were plotted as a function of antibody concentration (Fig. 2). It was generally noticed that the IC_{50} decreases (sensitivity increases) as the concentration of antibody and reaches its lowest value (highest possible sensitivity) when the concentration of anti- PD-L1 antibody was 20 ng mL^{-1} (Fig. 2). Accordingly, the subsequent experiments were conducted using PD-L1 protein and its antibody at concentrations of 0.1 μg mL^{-1} and 20 ng mL^{-1}, respectively.

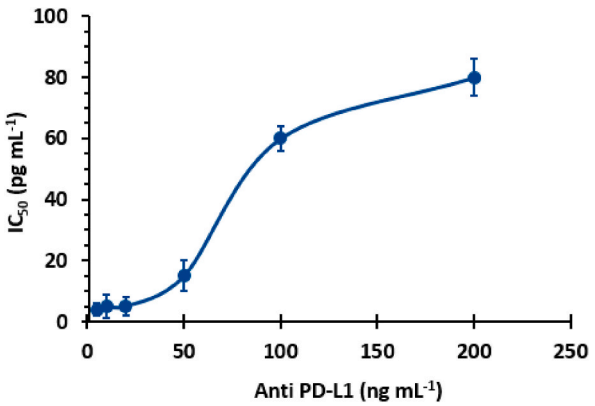

Fig. 2. The values of IC_{50} that were obtained by analysis conducted by using varying concentrations of anti- PD-L1 antibody in the assay. PD-L1 is the programmed death protein 1, and IC_{50} is the concentration of free soluble PD-L1 that cause 50 % inhibition of the maximum antibody binding to the immobilized PD-L1. The values are means of 3 determinations ± SD.

3.2.3. Selection of FITC-IgG concentrations

In the analysis based on KinExA, it is crucial to ensure that the net signal, which is generated by the antigen-antibody binding reaction, is both above zero and reasonably reproducible. Ideally, the net signal should fall within the range of 0.5–1.5 V [40]. To determine the most suitable concentration of FITC-IgG to achieve the desired signal, different concentrations of FITC-IgG (ranging from 0.05 to 1.25 μg mL^{-1}) were tested using a fixed concentration (5 pg mL^{-1}) of soluble PD-L1 (in the sample). The signals, after subtracting the background signals, were plotted against the concentration of FITC-IgG. The results demonstrated that the net signals increased with increasing concentrations of FITC-IgG, reaching a reasonably constant level when the concentrations were within the range of 1–2 μg mL^{-1} (Fig. 3). Beyond these concentrations, the signals decreased. Consequently, FITC-IgG concentration of 0.2 μg mL^{-1} was chosen for the assay.

The established optimal conditions, along with other optimized instrumental settings for running the KinExA system, were employed in the current assay. A summary of these conditions can be found in Table 1.

3.3. Validation of the assay

3.3.1. Binding curve and sensitivity

Using the established optimal conditions of the proposed KinExA, calibrator solutions of PD-L1 with varying concentrations (0.05–250 pg $mL^{-1)}$ were analyzed. The generated KinExAgram is given in Fig. 4. From the data, the binding calibration curve was generated to determine the concentration of PD-L1. The values of binding (%) were plotted against the corresponding PD-L1 concentrations (Fig. 5). The data was subjected to fitting by 4-parameter equation, and the results showed a very good correlation as the correlation coefficient was 0.9992. The working range of the assay, defined as the concentration range of PD-L1 giving binding in the range of 10–90 % of the maximum binding, was 0.5–100 pg mL^{-1}.

The limits of detection (LOD) and limits of quantification (LOQ) were calculated according to the guidelines of immunoassay validation of analytical procedures [41]. The LOD and LOQ were found to be 0.15 and 0.5 pg mL^{-1}, respectively. The calibration parameters are summarized in Table 2. It is wise to note that the high sensitivity of the KinExA allows for the determination of PD-L1 in very diluted plasma samples, as the reported baseline plasma levels of PD-L1 were >0.66 ng mL^{-1} (660 pg mL^{-1}) [25]. Additionally, Montemagno et al. [17] reported that the blood plasma cutoff point levels of the soluble PD-L1 in patients with metastatic clear cell renal cell carcinoma was 100 pg mL^{-1}. Masood et al. [21] reported that the mean plasma concentrations of PD-L1 in patients with glioblastoma multiforme was 48.98 ± 2.26 pg mL^{-1} compared to 27.63 ± 1.281 pg mL^{-1} in control group. Furthermore, Ando et al. [22] reported that the mean plasma concentrations of PD-L1 in patients with lung and gastric cancer treated with ICIs were 469.7 ± 298.8 and 323.0 ± 108.4 pg mL^{-1} in patients pre-treated with ICI and in control group, respectively. All these data verify the suitability of the KinExA assay in terms of the sensitivity for real-time applications in clinical settings.

3.3.2. Effect of plasma matrix

To ensure accurate quantitation of PD-L1 in plasma samples, it was important to investigate the impact of plasma matrix on KinExA accuracy. In this study, blank plasma samples were serially diluted in PBS, and each dilution was spiked with a known concentration of PD-L1. These spiked samples were analyzed using the established procedure of KinExA. The matrix effect was evaluated by calculating the recovery values. The obtained recovery percentages were plotted as a function of plasma dilutions (Fig. 6). It is evident that the recovery percentage increased with plasma dilution and levelled off at approximately 100 % when the plasma dilution was 32-fold. Accordingly, the plasma samples should be diluted at least 32 folds before their analysis by the proposed KinExA. It is wise to note that the reported baseline plasma levels of PD-L1 were >0.66 ng mL^{-1} (660 pg mL^{-1}) [25]. Accordingly, real plasma samples containing this concentration should be diluted at least 1320 folds to attain their PD-L1 concentrations within the working range of the

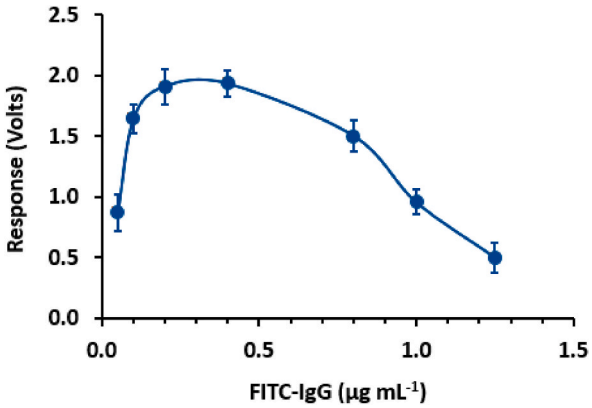

Fig. 3. The effect of fluorescein-labeled second antibody (FITC-IgG) concentration on the response signals for measurement of the immune complex of the programmed death protein 1 (PD-L1) with its antibody formed onto polymethylmethacrylate (PMMA) beads. The values are means of 3 determinations ± SD.

Table 1
Optimization of conditions for KinExA for measurement of PD-L1 in plasma.

Condition[a]	Value
Concentration of PD-L1 for beads coating (μg mL^{-1})	0.1
Coating conditions: time (h)/temperature (°C)	1/37
Concentration of BSA for beads blocking (%, w/v)	2
Blocking conditions: time (h)/temperature (°C)	1/37
Volume of beads suspension (μL)	583
Flow rate of beads suspension (mL min^{-1})	1
Concentration of anti- PD-L1 antibody (ng mL^{-1})	20
Sampling: volume (μL)/flow rate (mL min^{-1})	500/0.25
Concentration of FITC-IgG (μg mL^{-1})	0.2
FITC-IgG: volume (mL)/flow rate (mL min^{-1})	1/0.25

[a] Abbreviations are the following. PD-L1: the programmed death protein 1; BSA: bovine serum albumin; FITC-IgG: Fluorescein-labeled second antibody.

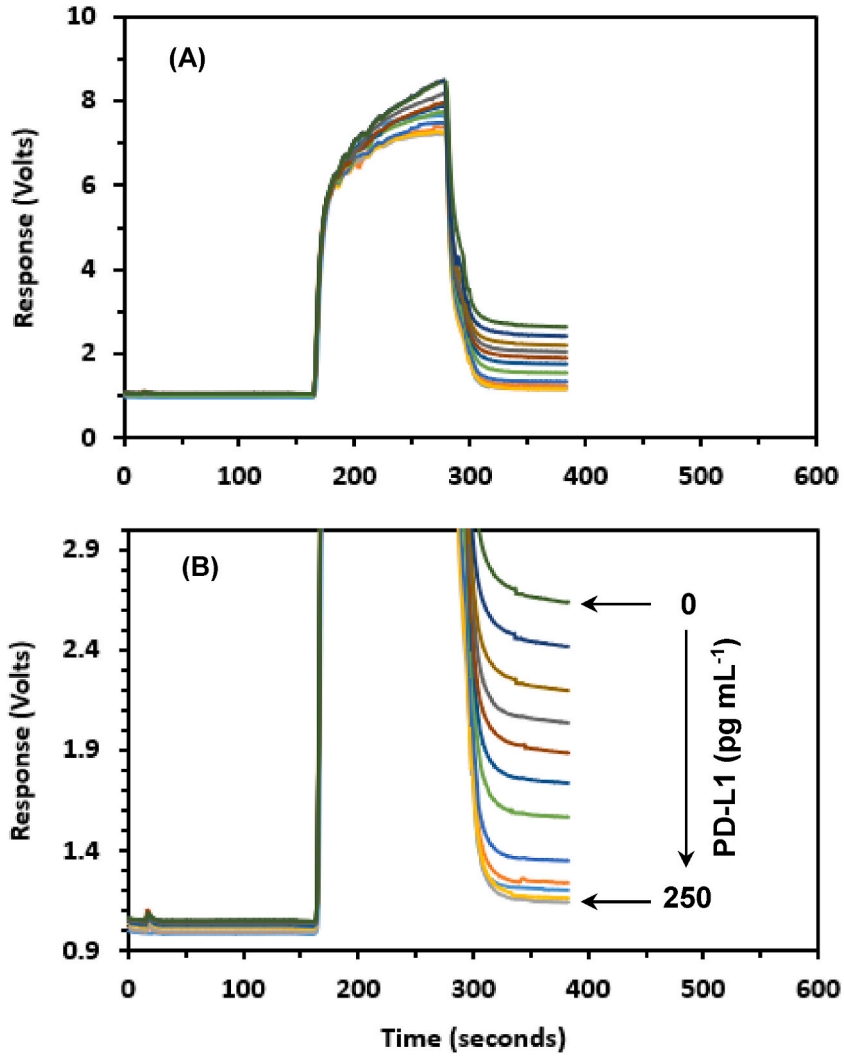

Fig. 4. Panel (A): Real time-response KinExAgram obtained by the KinExA™ instrument for varying concentrations of the programmed death protein 1 (PD-L1). Panel (B): The KinExagram data; however, they are presented on different scale of detector response (volts).

proposed KinExA (0.5–100 pg mL^{-1}). These results demonstrate the applicability of the assay for analyzing PD-L1 in plasma samples without any negative matrix effects on the assay results. Additionally, the high dilution of plasma samples required prior to analysis allows for the use of very small plasma volumes from patients, where only a few microliters of plasma will be sufficient for its analysis

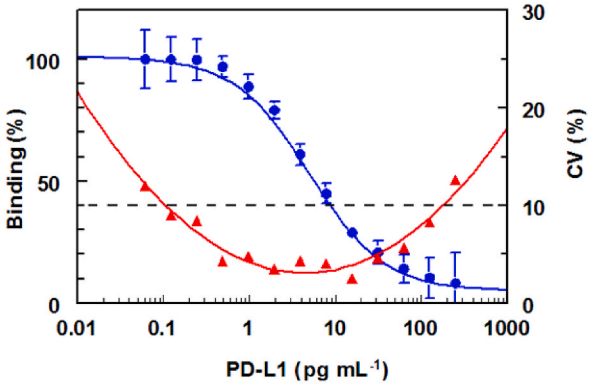

Fig. 5. Binding calibration curve (●) and its precision profiles (▲) of the proposed KinExA assay for measurement of the programmed death protein 1 (PD-L1) in plasma. CV (%) is the coefficient of variation, expressed as percentage. The values are means of 3 determinations ± SD.

Table 2
Results of calibration parameters of KinExA for measurement of PD-L1 in plasma.

Parameter	Value
Working range at binding of 10–90 % (pg mL^{-1})	0.5–100
4-Parameter equation correlation coefficient (r)	0.9992
Limit of detection, LOD (pg mL^{-1})	0.15
Limit of quantitation, LOQ (pg mL^{-1})	0.50

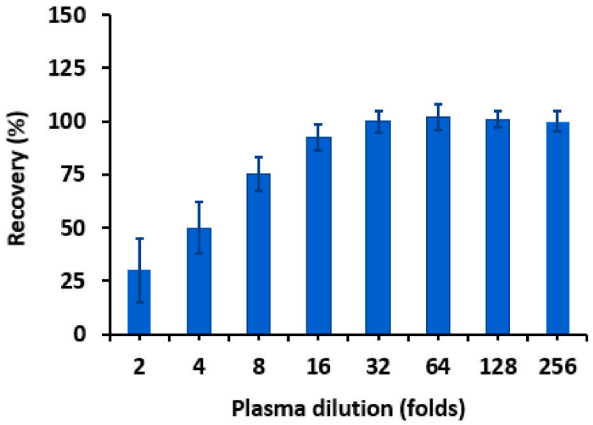

Fig. 6. Effect of plasma matrix on the recovery values for analysis of plasma samples containing PD-L1. The values are means of 3 determinations ± SD.

using the KinExA after its dilution. This feature makes the assay convenient for application in clinical laboratories, as it enables the use of minimal plasma samples. Additionally, this extreme sensitivity is important for future clinical application, particularly to follow patients undergoing adjuvant therapies or monitoring minimal residual cancer disease.

Table 3
Precision and accuracy of the proposed KinExA for PD-L1.

Spiked concentration (pg mL^{-1})	Recovery (% ± CV)	
	Intra-day	Inter-day
2	102.5 ± 5.4	96.4 ± 4.8
5	103.2 ± 3.8	101.2 ± 3.7
10	97.6 ± 3.9	104.3 ± 4.1
20	101.4 ± 4.8	98.6 ± 6.2

3.3.3. Precision and accuracy

The precision profile (coefficient of variation, CV%) obtained from the calibration samples is presented in Fig. 5. The values of CV (%) throughout the entire working range of the assay were consistently below 10 %, revealing good precision of the proposed KinExA. Additionally, the intra- and inter-day precisions of KinExA were assessed. For assessment of intra-day precision, PD-L1 samples of different concentrations (Table 3) were analyzed in triplicates within a single day. For inter-day precision, the same samples were analyzed in duplicate across three consecutive days. According to the recommendations of immunoassay validation [41], the proposed KinExA demonstrated satisfactory precision, as the CV (%) did not exceed 6.2 % (Table 3). The high precision of the proposed KinExA could be attributed primarily to the utilization of capturing PD-L1-coated beads with a high surface area which makes the assay precision mainly dependent on the concentrations of the anti- PD-L1 antibody and FITC-IgG, which are automatically dispensed with high precision by the KinExA biosensor.

To evaluate the accuracy of KinExA, the recovery of varying concentrations of PD-L1 (Table 3) spiked in plasma samples and subsequently diluted with PBS solution was determined. The obtained recovery values were in the range of 96.2 ± 4.8 % to 104.3 ± 4.2 % for the intra- and inter-day accuracy, respectively. These recovery values confirmed the accuracy of the assay for quantifying PD-L1 in plasma.

3.3.4. Comparison of the proposed KinExA with reported methodologies

The existing methodologies for measurements of soluble PD-L1 in plasma or serum include metal–organic framework-enhanced ELISA [29], SPR-based biosensor [30], SERS [31,32], and magnetic CLIA [33]. The KinExA described herein gave higher sensitivity (LOQ is 0.5 pg mL^{-1}) than ELISA (LOQ is 7.3 pg mL^{-1}). The increased sensitivity of KinExA compared to microwell plate-based ELISA and CLIA can be attributed to the inherent advantages of the KinExA method. In ELISA, a low concentration of anti-PD-L1 antibody (~equal to its dissociation constant, K), is typically used. As the concentration of the primary antibody decreases, the sensitivity increases, until reaching a maximum when the antibody concentration equals its K_D value [42]. Microwell-based ELISA and CLIA usually require a higher concentration of the primary anti-analyte antibody than the K_D value to achieve a detectable signal. However, in KinExA, even a very low concentration of antibody can generate adequate signal strength through accumulation from continuous sample flow. Additionally, the working conditions of KinExA, which involve a rapid flow of the pre-equilibrated mixture of PD-L1 and its antibody over the immobilized PD-L1 in the observation cell, prevent the dissociation of immune complexes. The immobilized PD-L1 served solely as a tool for separation and not as an effective competitor for antibody binding sites. This enables the detection of only free antibody molecules with unoccupied binding sites in the equilibrium mixture, leading to higher sensitivity. Furthermore, the response of KinExA sensor is dependent on the amount of antibody captured by PMMA-coated beads which have a larger surface area (260 mm^2) than that of microwell in ELISA (64 mm^2 per well) [43]. The increased surface area of the capturing beads in the KinExA format maximizes the opportunities for capturing more free antibodies, resulting in an improved quantifiable response with low signal-to-noise characteristics and acceptable reproducibility. Additionally, the proposed KinExA gave better sensitivity than SPR [30], whose LOQ was 5 pg mL^{-1}. SERS [31] gave better sensitivity (LOQ was 50 fg mL^{-1}) than our KinExA; however, the KinExA is more convenient than SERS which involved complicated fabrication and functioning of the sensor chip. As shown in Fig. 5 and Table 3, the present KinExA acceptable precision profile CV% was ≤6.2 %, compared to ≤12.5 % for the previous ELISA [29], and comparable precision with SERS (CV% was 3.65 %).

3.3.5. Assay throughput

The throughput of the KinExA assay enables efficient and high-capacity analysis of samples within a defined time frame. In principle, the KinExA platform offers several advantages in terms of sample processing and analysis speed, making it suitable for both small-scale and large-scale studies. The assay employed a flow-based technique, which allows for rapid analysis of multiple samples. The automated workflow, combined with the use of fluids delivery system, enables efficient handling and processing of samples, minimizing manual intervention and reducing assay time. The exact throughput of the KinExA assay can vary depending on factors such as the specific instrument configuration, sample preparation procedures, and the number of samples being analyzed. However, the platform is designed to accommodate high sample throughput, making it well-suited for applications where large numbers of samples need to be processed in a time-efficient manner.

In the present assay, the typical sample run time on the standard KinExA instrument employed in the study was 400 s (6.67 min/sample). This means that the instrument can analyze ~9 samples/hour (i.e., 215 samples/24 h). This throughput capability is particularly beneficial for basic research studies, while this capability could be enhanced for clinical applications that require large-scale screening or profiling of patient samples. This can be achieved by using the KinExA autosampler and adaptability of 96-well format for the assay. Additionally, the KinExA system's software and data analysis capabilities contribute to the overall efficiency of the assay throughput. The software enables automated data acquisition, processing, and analysis, allowing for rapid generation of results and facilitating data interpretation. In summary, the KinExA assay offers a high throughput capability, allowing for the analysis of several hundred to thousands of samples within a defined time frame. The automated workflow, microfluidics, and software-driven data analysis contribute to the efficiency and scalability of the assay, making it suitable for both small-scale and large-scale studies.

3.3.6. Application limitations of the assay and future work

It is recognized that testing clinical samples from cancer patients would provide valuable insights into the performance of the assay in a real-world setting, and translation of research findings to practical applications. However, it is important to note that our laboratories, being in academic institutes, do not have direct access to patient samples due to ethical and logistical constraints, and potential challenges in assay implementation. It is acknowledged that the absence of data from cancer patients has been a limitation in

this study; however, the study primarily focused on developing and optimizing the analytical aspects of the assay to ensure its accuracy and reliability. Future work is currently planned to resolve the potential challenges associated with obtaining patient samples and the strategies employed to overcome these limitations. The potential application of the assay in real clinical setting will have significant implications of our findings in the context of personalized medicine and the monitoring of immunotherapy response. By providing a comprehensive overview of our future directions and considerations, we aim to enhance the understanding of the potential clinical implications of our assay and stimulate further research in this field.

3.3.7. The favourable use of KinExA assays for quantitative analysis of diverse analytes

The KinExA-based assays have proven to be highly sensitive and versatile in detecting and quantifying various molecules of interest across a wide range of applications [40,44–52]. These molecules encompass bacteria [44], chemotherapeutic drugs targeting tyrosine kinase inhibitors [45], therapeutic monoclonal antibodies [46], hormones [47], biomarkers associated with different diseases and conditions [40], opiates [48], environmental contaminants [49,50], food toxins [51], and heavy metals [52].

4. Conclusions

The present study represents the first report that describes the development and validation of a highly sensitive automated flow KinExA for the measurement of soluble PD-L1 levels in plasma, as a predictive and prognostic biomarker for responses to cancer patients to ICIs. The assay was able to accurately quantify PD-L1 at a concentration as low as 0.5 pg mL^{-1}. The KinExA exhibited three notable advantages. Firstly, it overcame the limitations of mass transport and mobility effects encountered in ELISA and SPR that can affect the accuracy of the measurements. Secondly, the use of automated sampling in KinExA analysis increased assay throughput and convenience. The proposed sensor holds great promise for the measurement of PD-L1, particularly when a more reliable and precise result is required.

CRediT authorship contribution statement

Ibrahim A. Darwish: Writing – review & editing, Validation, Supervision, Funding acquisition, Data curation, Conceptualization. **Waleed Alahmad:** Writing – original draft, Validation, Investigation, Formal analysis. **Rajendran Vinoth:** Writing – original draft, Validation, Methodology, Data curation.

Declaration of competing interest

The authors declare that they have no known competing financial interests or personal relationships that could have appeared to influence the work reported in this paper.

Acknowledgments

The authors would like to extend their appreciation to the Researchers Supporting Project Number (RSPD2024R944), King Saud University, Riyadh, Saudi Arabia, for funding of this work.

References

[1] C. Robert, A decade of immune-checkpoint inhibitors in cancer therapy, Nat. Commun. 11 (2020) 3801.
[2] C. Blank, T.F. Gajewski, A. Mackensen, Interaction of PD- L1 on tumor cells with PD-1 on tumor- specific T cells as a mechanism of immune evasion: implications for tumor immunotherapy, Cancer Immunol. Immunother. 54 (2005) 307–314.
[3] N. Patsoukis, Q. Wang, L. Strauss, V.A. Boussiotis, Revisiting the PD-1 pathway, Sci. Adv. 6 (2020) eabd2712.
[4] H. Ledford, H. Else, M. Warren, Cancer immunologists scoop medicine Nobel prize, Nature 562 (2018) 20–21.
[5] Q. Gou, C. Dong, H. Xu, B. Khan, J. Jin, Q. Liu, J. Shi, Y. Hou, PD-L1 degradation pathway and immunotherapy for cancer, Cell Death Dis. 11 (2020) 955.
[6] Y. Iwai, M. Ishida, Y. Tanaka, T. Okazaki, T. Honjo, N. Minato, Involvement of PD- L1 on tumor cells in the escape from host immune system and tumor immunotherapy by PD- L1 blockade, Proc. Natl. Acad. Sci. USA 99 (2002) 12293–12297.
[7] G.T. Gibney, L.M. Weiner, M.B. Atkins, Predictive biomarkers for checkpoint inhibitor-based immunotherapy, Lancet Oncol. 17 (2016) e542–e551.
[8] M.Y. Teo, K. Seier, I. Ostrovnaya, A.M. Regazzi, B.E. Kania, M.M. Moran, et al., Alterations in DNA damage response and repair genes as potential marker of clinical benefit from PD-1/PD-L1 blockade in advanced urothelial cancers, J. Clin. Oncol. 36 (2018) 1685–1694.
[9] V. Gopalakrishnan, C.N. Spencer, L. Nezi, A. Reuben, M.C. Andrews, T.V. Karpinets, et al., Gut microbiome modulates response to anti-PD-1 immunotherapy in melanoma patients, Science 359 (2018) 97–103.
[10] D.T. Le, J.N. Durham, K.N. Smith, H. Wang, B.R. Bartlett, L.K. Aulakh, et al., Mismatch repair deficiency predicts response of solid tumors to PD-1 blockade, Science 357 (2017) 409–413.
[11] S.L. Topalian, F.S. Hodi, J.R. Brahmer, S.N. Gettinger, D.C. Smith, D.F. McDermott, et al., Safety, activity, and immune correlates of anti- PD-1 antibody in cancer, N. Engl. J. Med. 366 (2012) 2443–2454.
[12] R.S. Herbst, J.-C. Soria, M. Kowanetz, G.D. Fine, O. Hamid, M.S. Gordon, et al., Predictive correlates of response to the anti- PD-L1 antibody MPDL3280A in cancer patients, Nature 515 (2014) 563–567.
[13] FDA: US Food and Drug Administration, List of cleared or approved companion diagnostic devices (in vitro and imaging tools), Available at: https://www.fda.gov/medicaldevices/vitro-diagnostics/list-cleared-or-approvedcompanion-diagnostic-devices-vitro-and-imaging-tools. (Accessed 15 November 2023).
[14] FDA: US Food and Drug Administration, Summary of safety and effectiveness data (SSED) for PD- L1 IHC 28-8 pharmDx, Available at: http://www.accessdata.fda.gov/cdrh_docs/pdf15/p150025b.pdf. (Accessed 15 November 2023).
[15] FDA: US Food and Drug Administration, Summary of safety and effectiveness data (SSED) for VENTANA PD- L1 (SP142) assay, Available at: http://www.accessdata.fda.gov/cdrh_docs/pdf16/p160006b.pdf. (Accessed 15 November 2023).

[16] M.J. Duffy, J. Crown, Biomarkers for predicting response to immunotherapy with immune checkpoint inhibitors in cancer patients, Clin. Chem. 65 (2019) 1228–1238.
[17] C. Montemagno, A. Hagege, D. Borchiellini, B. Thamphya, O. Rastoin, D. Ambrosetti, J. Iovanna, N. Rioux-Leclercq, C. Porta, S. Negrier, et al., Soluble forms of PD-L1 and PD-1 as prognostic and predictive markers of sunitinib efficacy in patients with metastatic clear cell renal cell carcinoma, Oncoimmunol 9 (2020) 1846901.
[18] X. Zhu, J. Lang, Soluble PD-1 and PD-L1: predictive and prognostic significance in cancer, Oncotarget 8 (2017) 97671–97682.
[19] R. Ohkuma, K. Ieguchi, M. Watanabe, D. Takayanagi, T. Goshima, R. Onoue, K. Hamada, Y. Kubota, A. Horiike, T. Ishiguro, et al., Increased plasma soluble PD-1 concentration correlates with disease progression in patients with cancer treated with anti-PD-1 antibodies, Biomedicines 9 (2021) 1929.
[20] R. Fu, C.-Q. Jing, X.-R. Li, Z.-F. Tan, H.-J. Li, Prognostic significance of serum PD-L1 level in patients with locally advanced or metastatic esophageal squamous cell carcinoma treated with combination cytotoxic chemotherapy, Cancer Manag. Res. 13 (2021) 4935–4946.
[21] A.B. Masood, S. Batool, S.N. Bhatti, A. Ali, M. Valko, K. Jomova, K. Kuca, Plasma PD-L1 as a biomarker in the clinical management of glioblastoma multiforme-a retrospective cohort study, Front. Immunol. 14 (2023) 1202098.
[22] K. Ando, K. Hamada, M. Watanabe, R. Ohkuma, M. Shida, R. Onoue, Y. Kubota, H. Matsui, T. Ishiguro, Y. Hirasawa, H. Ariizumi, J. Tsurutani, K. Yoshimura, T. Tsunoda, S. Kobayashi, S. Wada, Plasma levels of soluble PD-L1 correlate with tumor regression in patients with lung and gastric cancer treated with immune checkpoint inhibitors, Anticancer Res. 39 (2019) 5195–5201.
[23] S. Ugurel, D. Schadendorf, K. Horny, A. Sucker, S. Schramm, J. Utikal, C. Pföhler, R. Herbst, B. Schilling, C. Blank, J.C. Becker, A. Paschen, L. Zimmer, E. Livingstone, P.A. Horn, V. Rebmann, Elevated baseline serum PD-1 or PD-L1 predicts poor outcome of PD-1 inhibition therapy in metastatic melanoma, Ann. Oncol. 31 (2020) 144–152.
[24] W. Qing V. So, D. Dejardin, E. Rossmann, J. Charo, Predictive biomarkers for PD-1/PD-L1 checkpoint inhibitor response in NSCLC: an analysis of clinical trial and real-world data, J. ImmunoTher. Cancer 11 (2023) e006464.
[25] L. Incorvaia, D. Fanale, G. Badalamenti, C. Porta, D. Olive, I. De Luca, C. Brando, M. Rizzo, C. Messina, M. Rediti, A. Russo, V. Bazan, J.L. Iovanna, Baseline plasma levels of soluble PD-1, PD- L1, and BTN3A1 predict response to nivolumab treatment in patients with metastatic renal cell carcinoma: a step toward a biomarker for therapeutic decisions, OncoImmunology 9 (2020) 1832348.
[26] S.Y. Oh, S. Kim, B. Keam, T.M. Kim, D.-W. Kim, D.S. Heo, Soluble PD-L1 is a predictive and prognostic biomarker in advanced cancer patients who receive immune checkpoint blockade treatment, Sci. Rep. 11 (2021) 19712.
[27] U. Krafft, C. Olah, H. Reis, C. Kesch, C. Darr, V. Grünwald, S. Tschirdewahn, B. Hadaschik, O. Horvath, I. Kenessey, et al., High serum PD-L1 levels are associated with poor survival in urothelial cancer patients treated with chemotherapy and immune checkpoint inhibitor therapy, Cancers 13 (2021) 2548.
[28] S. Jeong, N. Lee, M.-J. Park, K. Jeon, W. Song, Currently used laboratory methodologies for assays detecting PD-1, PD-L1, PD-L2 and soluble PD-L1 in patients with metastatic breast cancer, Cancers 13 (2021) 5225.
[29] S. Zhand, A. Razmjou, S. Azadi, S.R. Bazaz, J. Shrestha, M.A.F. Jahromi, M.E. Warkiani, Metal–organic framework-enhanced ELISA platform for ultrasensitive detection of PD-L1, ACS Appl. Bio Mater. 3 (2020) 4148–4158.
[30] B. Luo, Y. Wang, H. Lu, S. Wu, Y. Lu, S. Shi, L. Li, S. Jiang, M. Zhao, Label-free and specific detection of soluble programmed death ligand-1 using a localized surface plasmon resonance biosensor based on excessively tilted fiber gratings, Opt Express 10 (2019) 5136–5148.
[31] K.K. Reza, A.A.I. Sina, A. Wuethrich, Y.S. Grewal, C.B. Howard, D. Korbie, M. Trau, A SERS microfluidic platform for targeting multiple soluble immune checkpoints, Biosens. Bioelectron. 126 (2019) 178–186.
[32] Y. Pang, J. Shi, X. Yang, C. Wang, Z. Sun, R. Xiao, Personalized detection of circling exosomal PD-L1 based on Fe_3O_4@TiO_2 isolation and SERS immunoassay, Biosens. Bioelectron. 148 (2020) 111800.
[33] M. Goto, K. Chamoto, K. Higuchi, S. Yamashita, K. Noda, T. Iino, M. Miura, T. Yamasaki, O. Ogawa, M. Sonobe, H. Date, J. Hamanishi, M. Mandai, Y. Tanaka, S. Chikuma, R. Hatae, M. Muto, S. Minamiguchi, N. Minato, T. Honjo, Analytical performance of a new automated chemiluminescent magnetic immunoassays for soluble PD-1, PD-L1, and CTLA-4 in human plasma, Sci. Rep. 9 (2019) 10144.
[34] Sapidyne. KinExA Technology. Available at: https://www.sapidyne.com/. Accessed: November. 15, 2023.
[35] I.A. Darwish, Z. Wang, R.J. Darling, Development and comparative evaluation of two highly sensitive immunosensor platforms for trace determination of copper ions in drinking water using a monoclonal antibody specific to copper-EDTA complex, Molecules 28 (2023) 7017.
[36] I.A. Darwish, Z. Wang, R.J. Darling, N.Z. Alzoman, Development of two highly sensitive and selective sensor-assisted fluorescence immunoassays for trace determination of copper residues in food samples, RSC Adv. 13 (2023) 29195.
[37] I.A. Darwish, H. AlRabiah, M.A. Hamidaddin, Development of two different formats of heterogeneous fluorescence immunoassay for bioanalysis of afatinib by employing fluorescence plate reader and KinExA 3200 immunosensor, Sci. Rep. 9 (2019) 14742.
[38] M.A. Hamidaddin, H. AlRabiah, I.A. Darwish, Development and comparative evaluation of two immunoassay platforms for bioanalysis of crizotinib: a potent drug used for the treatment of non-small cell lung cancer, Talanta 201 (2019) 217–225.
[39] I.A. Darwish, T.A. Wani, A.M. Alanazi, M.A. Hamidaddin, S. Zargar, Kinetic-exclusion analysis-based immunosensors versus enzyme-linked immunosorbent assays for measurement of cancer markers in biological specimens, Talanta 111 (2013) 13–19.
[40] I.A. Darwish, T.A. Wani, A.M. Alanazi, M.A. Hamidaddin, S. Zargar, Kinetic exclusion analysis-based immunosensors versus enzyme-linked immunosrbent assays for measurement of cancer markers in biological specimens, Talanta 111 (2013) 13–19.
[41] J.W. Findlay, W.C. Smith, J.W. Lee, G.D. Nordblom, I. Das, B.S. DeSilva, M.N. Khan, R.R. Bowsher, Validation of immunoassays for bioanalysis: a pharmaceutical industry perspective, J. Pharm. Biomed. Anal. 21 (2000) 1249–1273.
[42] N. Ohmura, S.J. Lackie, H. Saiki, An immunoassay for small analytes with theoretical detection limits, Anal. Chem. 73 (2001) 3392.
[43] R.C. Blake II, A.R. Pavlov, D.A. Blake, Automated kinetic exclusion assays to quantify protein binding interactions in homogeneous solution, Anal. Biochem. 272 (1999) 123.
[44] F. Su, Y. Endo, H. Saiki, X.-H. Xiang, N. Ohmura, Simple and sensitive bacterial quantification by a flow-based kinetic exclusion fluorescence immunoassay, Biosens. Bioelectron. 22 (2007) 2500–2507.
[45] I.A. Darwish, H. AlRabiah, M.A. Hamidaddin, Development of two different formats of heterogeneous fluorescence immunoassay for bioanalysis of afatinib by employing fluorescence plate reader and KinExA 3200 immunosensor, Sci. Rep. 9 (2019) 14742.
[46] H. AlRabiaha, M.A. Hamidaddin, I.A. Darwish, Automated flow fluorescent noncompetitive immunoassay for measurement of human plasma levels of monoclonal antibodies used for immunotherapy of cancers with KinExA™ 3200 biosensor, Talanta 192 (2019) 331–338.
[47] N. Ohmura, S.J. Lackie, H. Saiki, An immunoassay for small analytes with theoretical detection limits, Anal. Chem. 73 (2001) 3392–3399.
[48] M.E. Eldefrawi, N.L. Azer, N. Nath, N.A. Anis, M.S. Bangalore, K.P. O'Connell, R.P. Schwartz, J. Wright, A sensitive solid phase fluoroimmunoassay for detection of opiates in urine, Appl. Biochem. Biotechnol. 87 (2000) 25–35.
[49] K. Camargo, M.A. Vogelbein, J.A. Horney, T.M. Dellapenna, A.H. Knap, J.L. Sericano, T.L. Wad, T.J. McDonald, W.A. Chiu, M.A. Unger, Biosensor applications in contaminated estuaries: implications for disaster research response, Environ. Res. 204 (2022) 111893.
[50] H.-J. Kim, W.L. Shelver, E.-C. Hwang, T. Xu, Q.X. Li, Automated flow fluorescent immunoassay for part per trillion detection of the neonicotinoid insecticide thiamethoxam, Anal. Chim. Acta 571 (2006) 66–73.
[51] B. Prieto-Simón, I. Karube, H. Saiki, Sensitive detection of ochratoxin A in wine and cereals using fluorescence-based immunosensing, Food Chem. 135 (2012) 1323–1329.
[52] I.A. Darwish, Z. Wang, R.J. Darling, Development and comparative evaluation of two highly sensitive immunosensor platforms for trace determination of copper ions in drinking water using a monoclonal antibody specific to copper-EDTA complex, Molecules 28 (2023) 7017.